Giant electrocaloric effect in thin film PbZr$_{0.95}$Ti$_{0.05}$O$_3$

A. Mischenko[1,*], Q. Zhang[2], J.F. Scott[3], R.W. Whatmore[2], and N.D. Mathur[1]

[1] *Department of Materials Science, Pembroke Street,*
University of Cambridge, CB2 3QZ, Cambridge, United Kingdom
[2] *Department of Advanced Materials, SIMS, Cranfield University, Beds MK43 0AL, United Kingdom and*
[3] *Centre for Ferroics, Earth Sciences Department,*
University of Cambridge, Cambridge CB2 3EQ, United Kingdom

An applied electric field can reversibly change the temperature of an electrocaloric material under adiabatic conditions, and the effect is strongest near phase transitions. This phenomenon has been largely ignored because only small effects [1] (0.003 K V^{-1}) have been seen in bulk samples such as Pb$_{0.99}$Nb$_{0.02}$(Zr$_{0.75}$Sn$_{0.20}$Ti$_{0.05}$)$_{0.98}$O$_3$ and there is no consensus on macroscopic models [2]. Here we demonstrate a giant electrocaloric effect (0.48 K V^{-1}) in 300 nm sol-gel PbZr$_{0.95}$Ti$_{0.05}$O$_3$ films [3] near the ferroelectric Curie temperature of 222°C. We also discuss a solid state device concept for electrical refrigeration that has the capacity to outperform Peltier or magnetocaloric coolers. Our results resolve the controversy surrounding macroscopic models of the electrocaloric effect and may inspire *ab initio* calculations of electrocaloric parameters and thus a targeted search for new materials.

I. INTRODUCTION

There has been increasing interest in novel cooling technologies over the last decades for several reasons. Firstly, it is important to reduce greenhouse gases that are used heavily in domestic and industrial refrigeration. Secondly, higher current densities in integrated circuits will impose higher demands on cooling systems that cannot be exclusively met by the current fan-based solutions. Thirdly, new requirements such as fibre optic lasers are continuously emerging. The electrocaloric (EC) effect in ferroelectrics generated great interest [1, 4, 5, 6] primarily in the 1950s-70s, but it has not been exploited commercially.

Small EC effects were reported in previous works by direct and indirect measurements that were in close agreement [1, 4, 7]. For example, bulk Pb$_{0.99}$Nb$_{0.02}$(Zr$_{0.75}$Sn$_{0.20}$Ti$_{0.05}$)$_{0.98}$O$_3$ shows the highest EC effect measured so far, and the direct measurements of the peak value (2.5 K in 30 kV cm^{-1}) were only 10-15% less than the indirect measurements [1, 7]. This work reports our discovery of a giant EC effect of 12 K in antiferroelectric thin films of Zr rich Pb(Zr,Ti)O$_3$ (PZT).

Microscopic theoretical treatments of the EC effect have not been forthcoming because the macroscopic theory is unestablished. Three leading textbooks on ferroelectricity differ on the macroscopic physics of the EC effect [8, 9, 10]. Fatuzzo and Merz [8] argue that the EC effect only occurs above the phase transition (Curie) temperature T_C, where the polarization P is finite in the presence of the applied electric field E. Mitsui, Tatsuzaki and Nakamura [9] argue that the EC effect can only occur below T_C, where the spontaneous value of P changes with temperature. Jona and Shirane [10] disagree with both [8] and [9], and assert that the effect occurs both

above and below T_C but is larger above. More generally, microscopic models of ferroelectrics are not well established. For example, it is only in the last decade that a fully quantum mechanical treatment has been available [11, 12].

We emphasise that there are no atomic-level *ab initio* models for the electrocaloric effect. This may be partly because of the confused macroscopic physics discussed above, and also because it has been difficult to carry out *ab initio* calculations for finite fields. However, in the past few months, Wu *et al.* [13] have managed to treat some materials, including BaTiO$_3$, in finite fields at absolute zero. It is our hope that the present work will encourage *ab initio* calculations of the electrocaloric effect. This will require further improvements because both finite temperatures and fields are necessarily involved.

II. ZIRCONIUM RICH PZT THIN FILMS

It is plausible that antiferroelectric thin films of Zr-rich PZT show promising EC effects, since the converse effect of pyroelectricity is pronounced and forms the basis of infrared detectors [14]. Both Zr-rich PZT and the more common compositions such as PbZr$_{0.48}$Ti$_{0.52}$O$_3$ are used both as capacitors due to their high dielectric constants [15], and also as high-strain actuators/transducers and prototype microelectromechanical systems due to their piezoelectric properties [15]. However, the potential for antiferroelectric films in cooling applications has not been considered.

Bulk Pb(Zr$_{0.95}$Ti$_{0.05}$)O$_3$ is an orthorombic antiferroelectric at room temperature. On heating to ~120°C, this structure transforms to a rhombohedral ferroelectric phase. There is substantial thermal hysteresis in this antiferroelectric to ferroelectric transition, which on cooling occurs at ~80°C. The structure transforms to cubic paraelectric above 242°C. This is a first-order phase transition with a Curie-Weiss temperature, extrap-

olated linearly from the inverse dielectric susceptibility, of T_o=225°C [16]. The rhombohedal to paraelectric transition at this composition is close to a tricritical point at PbZr$_{0.94}$Ti$_{0.06}$O$_3$ where its character changes from first to second order [17]. These transition temperatures, which were taken from single crystals and high purity ceramics, differ somewhat from much earlier data [3], in which the sample purity was not as great. The EC effect could not be predicted from the literature, since there is no data for Zr-rich PZT thin films at the high temperatures and high electric fields of interest.

III. EXPERIMENTAL

PZT sols were prepared from Sigma-Aldrich precursors. Pb(OAc)$_2$3H$_2$O was dissolved in methanol and refluxed for 2 hours at 70^{o}C. Separately, a mixture of acetic acid and methanol was added to a mixture of Zr(O^{n}Pr)$_4$ and Ti(O^{n}Bu)$_4$ and the resulting solution was stirred at room temperature for two hours. The Pb and Zr/Ti based solutions were mixed with a 20% excess of the former to compensate for Pb loss during sintering. After gentle stirring, the yellow solution obtained was passed through a 0.2 μm filter and stabilized by the addition of ethylene glycol.

Sols were spin-coated at 3000 rpm for 30 s onto Pt(111)/TiO$_x$/SiO$_2$/Si(100) substrates that had been rinsed with acetone and propanol. Layers of $\sim$70 nm were obtained by pre-firing in air on a hotplate at 300°C for 60 s, and then further annealing on another hotplate at 650°C for 10 minutes. This procedure was repeated five times to obtain $\sim$300 nm films.

Film structure was determined by x-ray diffraction on a Philips diffractometer using Cu Kα radiation. θ-2θ scans corresponded to a polycrystalline perovskite phase with no preferred orientations, and no traces of pyrochlore. Pt top electrodes of diameter 0.2 μm were sputtered deposited through a mechanical mask, and the bottom Pt electrode was contacted with silver dag at a substrate edge. The dielectric constant and loss tangent were measured using a HP 4192A Impedance Analyser at 100 kHz and 100 mV ac amplitude. Hysteresis measurements were carried out at 10 kHz using a Radiant Technologies Precision Premier workstation and a high temperature (280°C) probe station. The temperature of the sample was controlled via feedback from a thermocouple, accurate to 0.3^{o}C, in contact with the sample.

IV. RESULTS AND INTERPRETATION

Electrical hysteresis measurements were made roughly every $T = 15^o$C in the temperature range 35 - 280°C, on cooling to minimise reductions in P due to fatigue. Representative plots (Fig. 1) of $P(E)$ show the expected antiferroelectric behaviour [3] at 35°C, and at 280°C lossy paraelectric behaviour that in these mea-
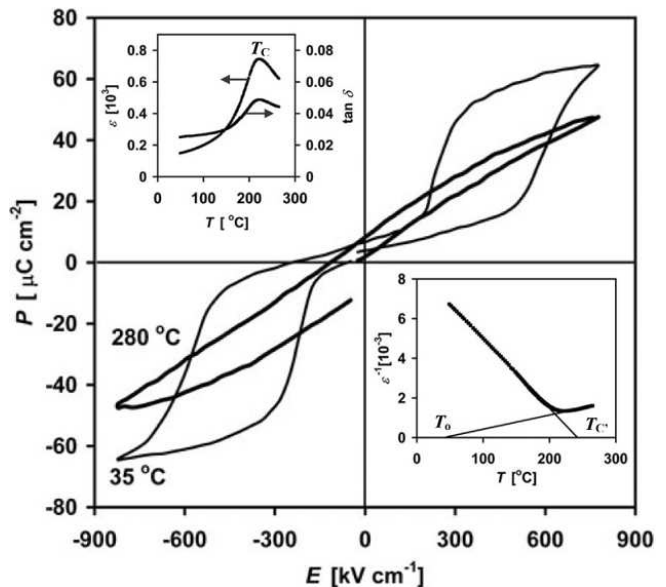

FIG. 1: Electrical measurements of Pb(Zr$_{0.95}$Ti$_{0.05}$)O$_3$ films on cooling. Polarisation P versus applied electric field E at 10 kHz showing evidence of antiferroelectricity at 35°C that persists up to 190°C. Above this temperature, we observe no qualitative change corresponding to the ferroelectric to paraelectric transition that is apparent from the insets. The data at 280°C shows lossy paraelectric behaviour. Upper inset: the real part of the effective dielectric constant measured at 100 kHz shows a single peak at the bulk phase change temperature $T_C = 222^o$C, below which the antiferroelectric-ferroelectric transition cannot be resolved. Loss tangent tan $\delta = 3\%$ at 35°C. Lower inset: extrapolation of the low temperature $1/\varepsilon$ data to zero gives $T_{C'} = 242^o$C, and the corresponding high temperature extrapolation gives the Curie-Weiss temperature $T_o \approx 40^o$C. Since $T_o < T_{C'}$, the ferroelectric-paraelectric transition is first order [19].

surements is indistinguishable from the ferroelectric loops at intermediate temperatures. The dielectric constant ε and loss tangent each show a broad peak associated with the ferroelectric-paraelectric transition at T_C=222°C on cooling (upper inset, Fig. 1) and T_C=215°C on heating, but no peaks corresponding to the antiferroelectric-ferroelectric transition can be resolved. This broadness is typical of thin films and is likely due to interfacial strain, scalar concentration gradients, or other forms of microscopic variability [18]. Reversible adiabatic changes in EC entropy S, energy U and temperature T for a material of density ρ with heat capacity C are given [7] by:

$$\Delta S = -\frac{1}{\rho} \int_{E_1}^{E_2} \left(\frac{\partial P}{\partial T} \right)_E dE, \tag{1}$$

$$\Delta U = -\frac{1}{\rho} \int_{E_1}^{E_2} T \left(\frac{\partial P}{\partial T} \right)_E dE, \quad \text{and} \tag{2}$$

$$\Delta T = -\frac{1}{\rho} \int_{E_1}^{E_2} \frac{T}{C} \left(\frac{\partial P}{\partial T} \right)_E dE, \tag{3}$$
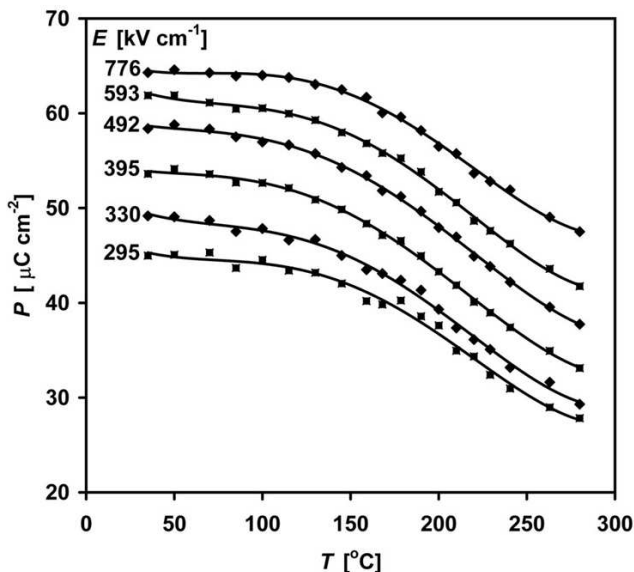
FIG. 2: The temperature dependence of polarisation P at selected applied fields E. Data extracted for $E > 0$ from the upper branches of nine hysteresis loops measured at 10 kHz in 35°C $\leq T \leq 280^{o}$C. The EC effect is largest when $|\partial P/\partial T|$ is maximised at the broad paraelectric to ferroelectric transition. The lines represent 4th order polynomial fits to the data.

FIG. 3: Electrocaloric entropy and energy changes. Main panel, entropy changes S were calculated from equation (1) using the fits presented in Fig. 1, at selected values of $E = E_2 - E_1$ with $E_2 = 776$ kV cm^{-1}. Inset, at $T = 220^{o}$C the EC energy U was similarly calculated from equation (2) as a function of $E = E_2 - E_1$, with $E_2 = 776$ kV cm^{-1}. The corresponding hysteresis losses as determined from the $P(E)$ loops (e.g. Fig. 1) are small. This justifies the indirect approach used to calculate the strength of the EC effect.

assuming the Maxwell relation $\partial P/\partial T = \partial S/\partial E$. Values of $\partial P/\partial T$ were obtained from 4th order polynomial fits to $P(T)$ data (Fig. 2). Fatigue may only reduce our values of $|\partial P/\partial T|$ since the data were taken on cooling such that P increased in successive hysteresis measurements. In the temperature range of interest, the heat capacity $C = 330$ J K^{-1} kg^{-1} remains sensibly constant for Zr rich PZT films, and the peak associated with the transition is $< 10\%$ of the background [20, 21]. We note that assuming a constant value of C despite a $\approx 50\%$ peak [7] resulted in excellent agreement with direct EC measurements of T in bulk Pb$_{0.99}$Nb$_{0.02}$(Zr$_{0.75}$Sn$_{0.20}$Ti$_{0.05}$)$_{0.98}$O$_3$ [1]. A value of $\rho = 8.3$ g cm^{-3} reported for the similar compound (Pb,Zr,Sn)TiO$_3$ was used here [7]. The lower integration limit $E_1 = 295$ kV cm^{-1} was set deliberately high to avoid the antiferroelectric regime (at low fields, Fig. 1), which ensures that $\partial P/\partial T < 0$. The upper integration limit $E_2 = 776$ kV cm^{-1} represents the maximum field at which a consistent dataset could be obtained.

EC entropy changes associated with the ferroelectric-paraelectric transition are shown in Fig. 3. At $E = 30$ kV cm^{-1}, the peak value of S is consistent with bulk values of 0.6 J K^{-1} kg^{-1} in Pb$_{0.99}$Nb$_{0.02}$(Zr$_{0.455}$Sn$_{0.455}$Ti$_{0.09}$)$_{0.98}$O$_3$ [4]. At larger fields, the peak value of S is significantly larger, and is comparable with values of ≈ 15 J K^{-1} kg^{-1} reported for the best magnetocaloric materials in large magnetic fields of 5 T [22, 23, 24]. Since hysteresis losses are at worst 5% of the EC energy changes (Fig. 3, inset), the reversible thermodynamics assumed here (equations 1-3) is a rea-
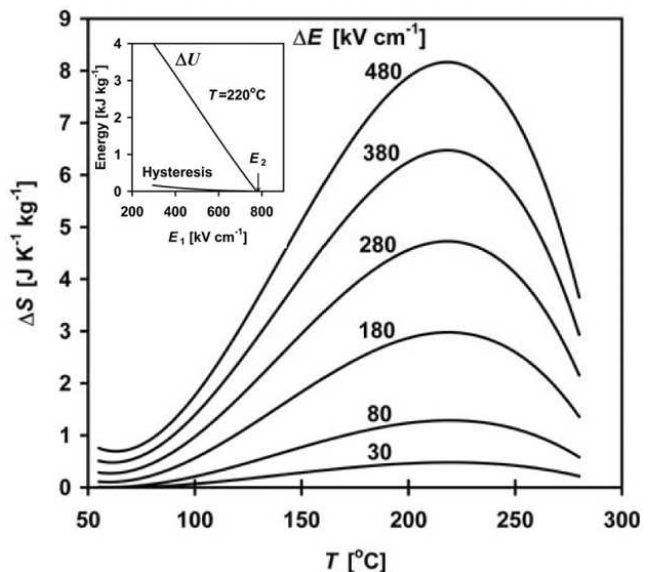
sonable approximation.

EC temperature changes corresponding to the entropy changes in Fig. 3 are presented in Fig. 4. The largest change (12°C in 25 V, i.e. 0.48 K V^{-1}) at $T_{EC} = 226^{o}$C dwarfs the previous best results obtained in bulk Pb$_{0.99}$Nb$_{0.02}$(Zr$_{0.75}$Sn$_{0.20}$Ti$_{0.05}$)$_{0.98}$O$_3$ (2.5^{o}C in 750 V, i.e. 0.003 K V^{-1}) at $T_{EC} = 162^{o}$C. At all electric fields studied, the effects persist both above and below $T_C = 222^{o}$C, unlike the models of [8] and [9], possibly because the transitions are not sharp in our films. The effect peaks at $T_C < T_{EC}$ supporting the model of [10], and since $T_{C'} = 242^{o}$C (lower inset, Fig. 1), we also have $T_C < T_{EC} < T_{C'}$ which implies that our data support the picture for first order phase transitions presented in [2].

We propose that the EC effect demonstrated here in Pb(Zr$_{0.95}$Ti$_{0.05}$)O$_3$ films may be exploited in an efficient solid state heat pump that two of us (A.M. and N.D.M.) proposed previously [25, 26]. In this design, thermoelectric heat switches such as Peltier units separate the EC element from the heat source and heat sink. Each switch is open when driven by a sufficiently large forward current. In the absence of this current the switch is closed and conducts heat passively. A reverse current enhances heat flow. Multiple EC elements with a range of working temperatures may be separated by heat switches in order to span larger temperature ranges.

A future challenge is to increase cooling power by increasing EC film thickness. Simulations assuming bulk
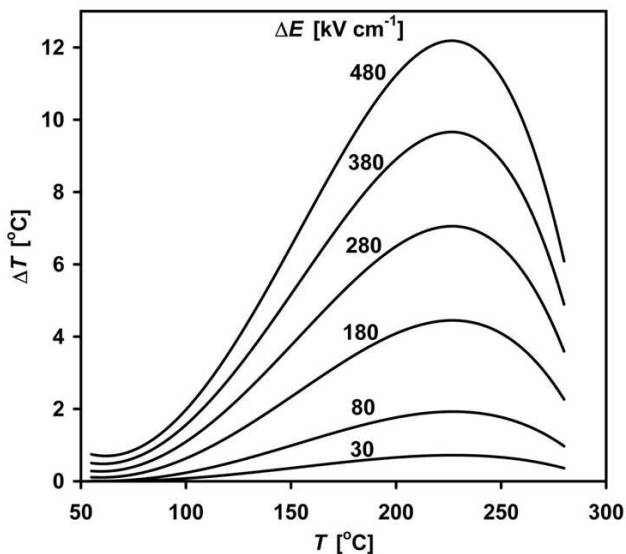
FIG. 4: Electrocaloric temperature changes. T was calculated from equation (3) using selected values of $E = E_2 - E_1$, with $E_2 = 776$ kV cm^{-1}. The peak value of 12°C occurs at $T_{EC} = 226^o$C with $E = 480$ kV cm^{-1}.

$Pb_{0.99}Nb_{0.02}(Zr_{0.75}Sn_{0.20}Ti_{0.05})_{0.98}O_3$ properties [7] represent lower bounds on performance. For a 6 K change across four such $30\times30\times2$ mm^3 EC elements, separated by $30\times30\times0.5$ mm^3 Bi_2Te_3 Peltier heat switches, we obtained at a device operating frequency of 10 Hz a coefficient of performance approaching $\approx$50% of the Carnot limit, i.e. a cooling power of $\approx$50 W for an input of several watts.

We now make a brief comparison with competing refrigeration technologies. Bulk magnetocaloric materials such as $Gd_5Ge_2Si_2$ (15 K in 5 T) [22] and $MnFeP_{0.45}As_{0.55}$ (4.2 K in 1.45 T) [24] show impressive effects, and the efficiency of a prototype cooling system is 60% of the Carnot limit [27]. However, the large magnetic fields required are impractical, whereas by contrast it is relatively simple to generate the large electric fields relevant to the EC effect. Electrically driven Peltier coolers [28] based on Bi_2Te_3 semiconductors are compact and cheap, but show [29] poor coefficients of performance, e.g. 3% for a cooling power of 15 W with $\Delta T = 10$ K.

The EC effect demonstrated here will hopefully inspire theoretical insights into ferroelectrics, materials improvements that involve e.g. doping [14, 30] or switching to bismuth-based ferroelectrics [31], and ultimately commercial applications. For example, the EC effect could provide cooling solutions for electronic components such as computer chips. The pyroelectric effect could be used for example to recover useful electrical power from waste heat. Indeed, we note that the optimisation of one effect necessarily optimises the other, and that stress free environments should be more attractive than the strain free environments experienced by the thin films.

[1] B. A. Tuttle and D. Payne, Ferroelectrics **37**, 603 (1981).
[2] J. Scott, Encyclopedia of applied physics, VCH, Berlin **5**, 1 (1993).
[3] E. Sawaguchi, J. Phys. Soc. Japan **8**, 615 (1953).
[4] P. D. Thacher, J. Appl. Phys. **39**, 1996 (1968).
[5] W. N. Lawless, Phys. Rev. B. **16**, 433 (1977).
[6] A. J. Morrow and W. N. Lawless, Ferroelectrics **15**, 159 (1977).
[7] B. A. Tuttle, Ph.D. thesis, University of Illinois at Urbana - Champaign (1981).
[8] E. Fatuzzo and W. J. Merz, *Ferroelectricity* (North-Holland, Amsterdam, 1967).
[9] T. Mitsui, *Introduction to the Physics of Ferroelectricity* (Gordon and Breach, London, 1976).
[10] F. Jona and G. Shirane, *Ferroelectric Crystals* (McMillan, NY, 1962).
[11] R. Resta, Rev. Mod. Phys. **66**, 899 (1994).
[12] R. D. Kingsmith and D. Vanderbilt, Phys. Rev. B. **47**, 1651 (1993).
[13] X. Wu, D. Vanderbilt, and D. R. Hamann, Phys. Rev. B. **72**, 035105 (2005).
[14] Q. Zhang and R. W. Whatmore, J. Appl. Phys. **94**, 5228 (2003).

[15] W. Y. Pan, C. Q. Dam, Q. M. Zhang, and L. E. Cross, J. Appl. Phys. **66**, 6014 (1989).
[16] R. Whatmore, Ph.D. thesis, University of Cambridge (1977).
[17] R. Whatmore, R. Clarke, and A. Glazer, J. Phys. C: Solid State Phys. **11**, 3089 (1978).
[18] M. M. Saad, P. Baxter, R. M. Bowman, J. Gregg, F. D. Morrison, and J. F. Scott, J. Phys.: Cond. Matt. **16**, L451 (2004).
[19] J. Scott, *Ferroelectric Memories* (Springer, Berlin, 2000).
[20] S. Davitadze, Ph.D. thesis, Lomonosov Moscow State University (2003).
[21] G. Suchanek, G. Gerlach, A. Deyneka, L. Jastrabik, S. Davitadze, and B. Strukov, Mat. Res. Soc. Proc. **D8.4.1**, 718 (2002).
[22] V. K. Pecharsky and K. A. Gschneidner, Phys. Rev. Lett. **78**, 4494 (1997).
[23] O. Tegus, E. Bruck, K. H. J. Buschow, and F. R. de Boer, Nature **415**, 150 (2002).
[24] E. Brck, M. Ilyn, A. M. Tishin, and O. Tegus, J. Magn. Magn. Mater. **290-291**, 8 (2005).
[25] A. S. Mischenko and N. D. Mathur, in *APS March Meeting* (Los Angeles, USA, 2005).

[26] A. S. Mischenko and N. D. Mathur, UK (0426230.9) and US (60/682,295) patents pending (2004).

[27] C. Zimm, A. Jastrab, A. Sternberg, V. Pecharsky, K. Gschneidner, M. Jr., Osborne, and I. Anderson, Adv. Cryog. Eng. **43**, 1759 (1998).

[28] H. J. Goldsmid, *Electronic refrigeration* (Pion Ltd., London, 1986).

[29] R. Otey and B. Moskowitz, SPIE magazine of photonics technologies and aplications **1, 3**, 34 (2001).

[30] Q. Zhang, J. Phys. D.: Appl. Phys. **37**, 98 (2004).

[31] D. Fu, K. Suzuki, and K. K., Jpn. J. App. Phys. **41**, L1103 (2002).